Measurement of the pressure waves generated in a high-speed train-tunnel model

Dong Hyeon Kim[1], Tae Hwan Ko[1], Tae Ho Kim[2], Heuy Dong Kim[2]*

[1] Korea Railroad Research Institute (KRRI), Uiwang, Republic of Korea

[2] Andong National University, Department of Mechanical Engineering, Andong, Republic of Korea

*kimhd@anu.ac.kr

Abstract

When a high speed train approaches a tunnel, a compression wave is formed in the tunnel entry. The compression wave propagates in the tunnel at a sonic speed. When it reaches the tunnel exit, the part of it is emitted as an impulse wave to the outside and the remainder is reflected into the tunnel as an expansion wave. The impulse wave emitted from the exit generates explosive noise and low frequency vibration, and causes serious environmental problems such as affecting the crack of private houses and buildings around the tunnel. In order to solve these problems, it is important to measure the pressure waves generated in the tunnel. In this study, a test bed for the train-tunnel system is constructed, and the characteristics of the compression wave propagating in the tunnel is investigated. As the results, the pressure rise due to the compression wave in the tunnel increased in proportion to the train speed.

1 Introduction

When a high speed train approaches a tunnel, the compression wave is formed in the tunnel entry with the piston effect of the train. The compression wave propagates in the tunnel at a sonic speed. When it reaches the tunnel exit, the part of it is emitted as an impulse wave to the outside and the remainder is reflected into the tunnel as an expansion wave. The impulse wave emitted from the exit generates an explosive noise and low frequency vibration, and causes serious environmental problems such as affecting the crack of private buildings and being discomfort to residents around the tunnel(Kim (1994)).

As the high-speed railway has recently become spreading, it is expected that the explosive noise will be generated at the tunnel exit by adopting a small cross-sectional tunnel and concreted slab track for cost reduction and easy maintenance. In order to solve these problems, it is very important to measure the characteristics of the compression wave and the impulse wave in the train-tunnel system.

Hara (1960) derived a formula for predicting the pressure rise in the tunnel by the initial compression wave. The pressure rise across the compression wave generated when a train enters a tunnel increases approximately as the square of the train speed. Based on the theory of acoustics, Aoki et al. (2000) and Baron et al. (2006) derived the relationship between the initial compression wave and the impulse wave at the tunnel exit. The peak value of an impulse wave emitted from the tunnel exit is proportional to the maximum pressure gradient of the compression wave at the tunnel entry. It was derived to be independent of the strength of the compression wave while depends on the length of compression wave.

In this study, a test bed for the train-tunnel system is constructed, and the characteristics of the initial compression wave propagating in the tunnel is investigated. The results of this study will provide important basic data for predicting and reducing the peak value of the impulse wave emitted from tunnel exit in future.

2 Experimental Methods

Figure 1: High speed train-tunnel test bed.

Field tests are costly and time consuming to investigate the effects of high-speed train speeds and the design changes of civil engineering facilities inside and outside the tunnel on the aerodynamic phenomena of train-tunnel system. To solve the problems, a reduced model was used. A test bed for high speed train-tunnel system is shown in Figure 1. The train-tunnel model driving tester can be classified into a launch part, a test part, and a braking part depending on the train model speed. The launch part is an air gun type, which uses a high pressure air to launch a stopped train model at high speed. The train model launched at high pressure accelerates and travels at the target speed in an air dissipation tank. In this study, a high speed train-tunnel test bed was constructed with a scale ratio of 1/64.2 for the real tunnel run test of Korean railway general test line.

Figure 2 shows the schematic of train-tunnel model for the high speed test bed. The train model is axisymmetric and the tunnel model is rectangular. According to the previous study(Fukuda et al. (2010)), the error range within 2 % was obtained in the comparison test of the pressure fluctuation in tunnel between 3D real shape and the axisymmetric train models. The direction of the train was controlled by applying a 3 mm diameter guide wire to the center of the train model. In order to minimize deflection and vibration of the wire while the train model was running, the guide wire was pulled just before the yield point.

The specifications of the real test line and the reduced model are shown in Table 1. The EMU-250 high-speed trains will be loaded on new routes of 200 km/h and 250 km/h, which were completed in 2017 and will be tested for trial operation. The blockage ratio (the cross-sectional area of the train divided by the cross-sectional area of the tunnel) used in this study is 0.2165.

In a high-speed train-tunnel system, aerodynamic phenomena are very complicated unsteady flows, so pressure measurement sensors with very high sensitivity are required to accurately measure pressure fluctuations over time. In this study, a gauge pressure sensor of ENDEVCO model 8510B-1 from MEFFITT Sensing System was used as a piezo-resistive sensor. The pressure sensor has a sensitivity of up to 250 mV/psi and has a measurement range of 6,895 Pa (1 psi), which is known to be measurable over a relatively wide frequency band including ultra-low frequencies. It has a satisfactory precision in measuring pressure fluctuations inside the tunnel. The resolution is 0.5 Pa. In addition, Keyence's photo sensors were applied to accurately measure the speed of the train model. Each photo and pressure sensor is connected to the data acquisition device by a signal cable, and all sensors are controlled by the Lab view program. Once the train model reaches the first photo sensor, all sensors installed in the train-tunnel model are programed to receive 25,000 physical signals at 0.00004 second interval for 1 second.

Figure 3 shows the locations of the pressure sensor for measuring the pressure fluctuations in the tunnel during train model travels. The pressure fluctuations inside the tunnel model were measured at the locations of 1,559 mm (corresponding to 100 m), 3,116 mm (200 m) and 4,672 mm (300 m) from the tunnel entrance. The pressure fluctuations were also measured at the locations of the equivalent diameter

D (125 mm), 3D (374 mm) and 3,116 mm (corresponding to 200m) from the tunnel exit to the inside. The train-tunnel model has a rectangular baffle plate of 600mm x 500mm at the entrance and exit.

In the test bed, the train model launch device is air gun type. High pressure air is injected into the air chamber to open the piston valve at the front end of the chamber at a high speed of 0.2 second or less to drive the train model. The piston valve always keeps the same opening speed. The launch speed of the train model can be adjusted according to the air pressure filled in the air chamber. This air pressure is called as the launching pressure. Calibration of the launching pressure and train model speed should be performed to drive the train model at the desired speed. The calibration of train model speed versus launching pressure is shown in Figure 4. The train model speed is the tunnel entry speed. In this study, all the experimental values are the mean values obtained from three repeated experiments at the same train
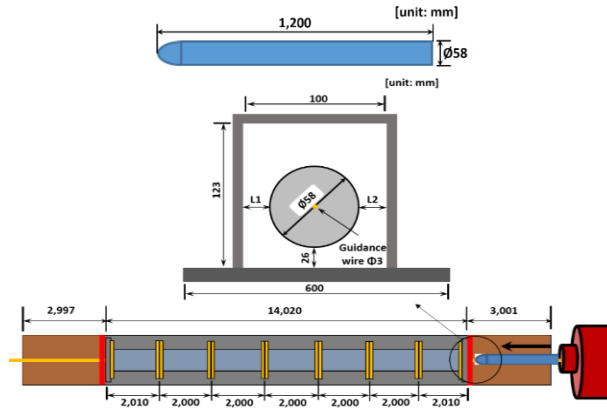

Figure 2: Schematic of high speed train-tunnel model.

speed.

Table 1: Specifications of the real test line and the reduced model

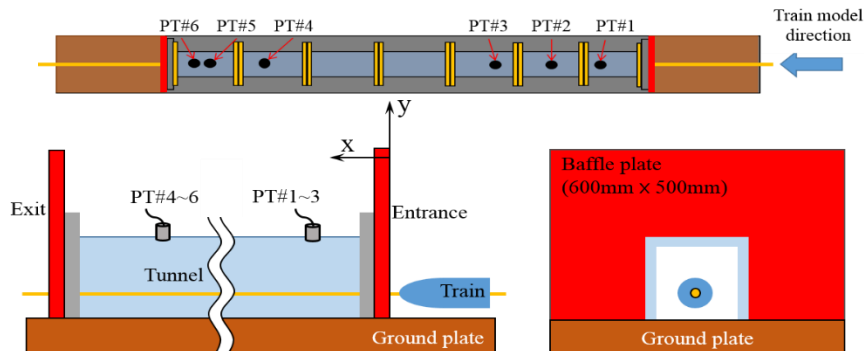| No.	Real test line	Model(1:64.2)
Train name	EMU-250	
Train cross area	10.89 m^2	2,642 mm^2
Tunnel cross area	50.3 m^2	12,204 mm^2
Blockage ratio	0.2165	
Train length	77.04 m	1,200 mm
Tunnel length	900 m	14,019 mm

Figure 3: Various measurement locations for compression wave.
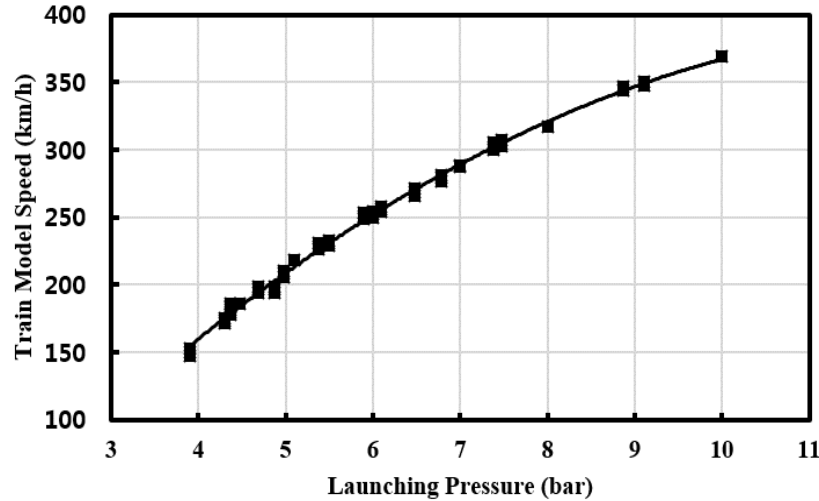
Figure 4: Relationship between train model speed and launching pressure.

3 Results and Discussion

When a train travels into a tunnel, complicated pressure fluctuations occur inside the tunnel. These pressure fluctuations are mainly caused by the interaction between the behavior of the pressure waves generated by the train and the traveling train in the tunnel. Figure 5 shows the pressure waveforms measured at the pressure measurement points (PT#1~PT#6) when the train model entry speed V is 250 km/h. The vertical dashed lines in the figure indicate that the train passes through the tunnel. In the figure, when the initial compression wave reaches the measurement point of PT#1, a sudden pressure rise occurs, then gradually increases to a maximum value and then decreases sharply. This pressure waveform is maintained until the measurement point of PT#4, and the waveform changes at the measurement points of PT#5 and PT#6. This is because the measurement points of PT#5 and PT#6 are located near the tunnel exit, so that the expansion wave reflected from the tunnel exit reaches. In the figure, the pressure fluctuation continues even after the train passes through the tunnel. This is due to the reflection of the pressure waves at the entrance and exit of tunnel, and it disappears over time.

Since the impulse wave emitted from the tunnel exit is closely related to the initial compression wave form, this study focuses on the initial compression wave in the pressure fluctuations shown in the figure 5. The symbols used to analyze the initial compression wave are shown in Figure 6. Figure 6(a) shows the pressure waveform and pressure gradient measured at the measurement point of PT#1 when the train entry speed is 250km/h. Figure 6(b) is schematic for the initial compression wave of the figure (a). In the figure, the point at which the pressure starts to increase from the atmospheric pressure, and the pressure gradient becomes almost constant after the sudden pressure rise, that is, the head and tail of the initial compression wave are denoted by point **a** and point **c**, respectively. Let the pressure Δp_{c1} at point **c** be the strength of the initial compression wave, and the time Δt_{ac} from point **a** to point **c** be the time it takes for the tail of the compression wave to reach after the head of compression wave arrives at the measurement point. Let **d** be the point at which the pressure increases and then decreases after the compression wave, and the pressure at that point is Δp_d, and the Δt_{ad} be the time from point **a** to point **d**. The **b** is the point at which the pressure gradient becomes maximum at the initial compression wave, and the maximum pressure gradient at that point b is $(d\Delta p/dt)_{max}$. Let **A** be the point at which the maximum pressure gradient meets the dashed line representing the atmospheric pressure, **B** be the point that the maximum pressure gradient meets the extension of the segment cd, and Δp_B be the pressure at point **B**.
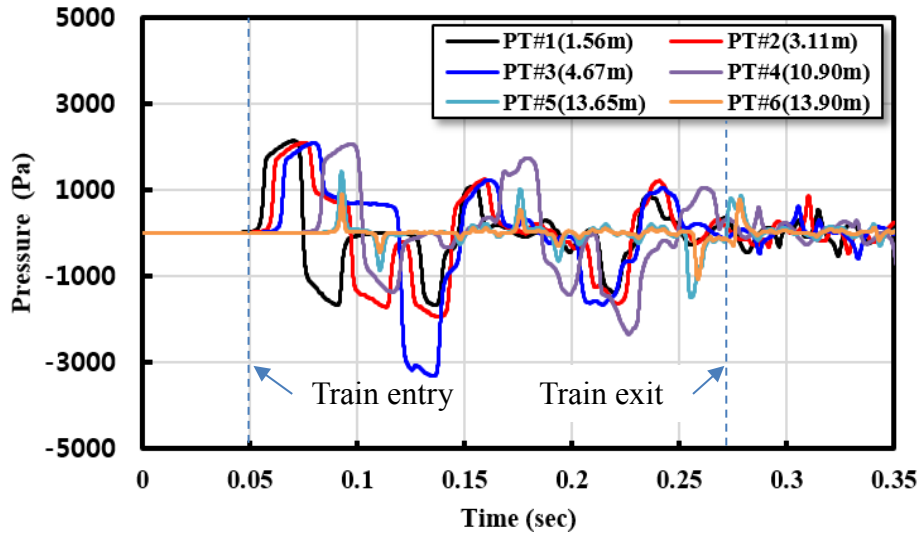
Figure 5: Pressure fluctuations in tunnel (V=250km/h).

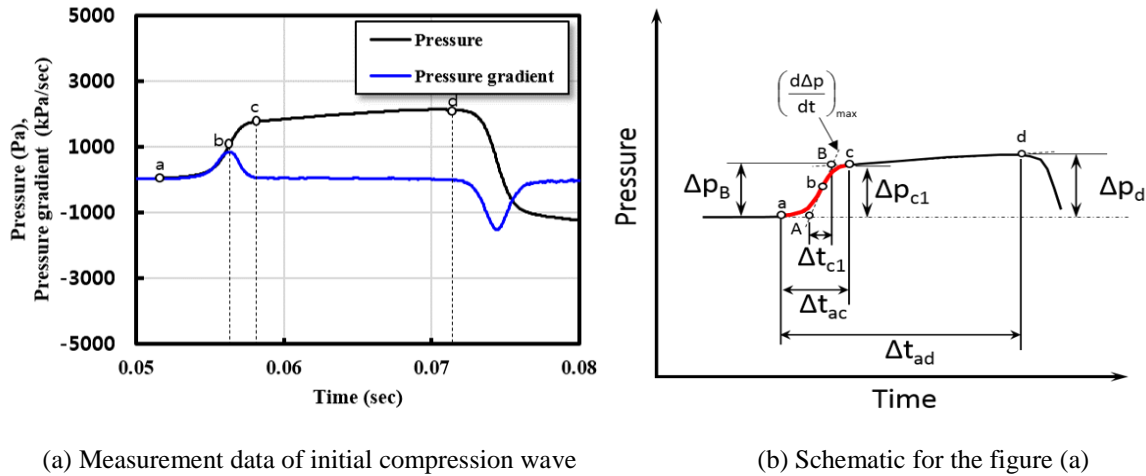(a) Measurement data of initial compression wave   (b) Schematic for the figure (a)

Figure 6: Symbols defined for initial compression wave analysis (PT#1, V=250km/h).

Hara (1960) derived the equation for predicting the pressure rise Δp_{c1} by the initial compression wave in the tunnel as follows.

$$\Delta p_{c1} = \frac{1}{2}\gamma p_1 M_t^2 \left[\frac{1-\phi^2}{\phi^2+(1-\phi^2)M_t-M_t^2}\right] \tag{1}$$

Where γ is the specific heat ratio of air, p_1 is the atmospheric pressure, M_t is the Mach number of the train($\equiv V/a_1$, a_1 is the sound speed in stationary air), and ϕ is the cross sectional area ratio($\equiv(A_1-A_2)/A_1$, A_1 and A_2 are the tunnel and train cross sections).

Figure 7 shows the initial compression wave strength according to the train entry speed. In the figure, the solid line is the theoretical value obtained from the equation of (1), and the symbol is the experimental value obtained from the compression waveform measured at the measurement point of PT#1. As the train entry speed increases, the compression wave strength also increases. As shown in the figure, the experimental and theoretical values of the compression strength agreed well with the train entry speed.
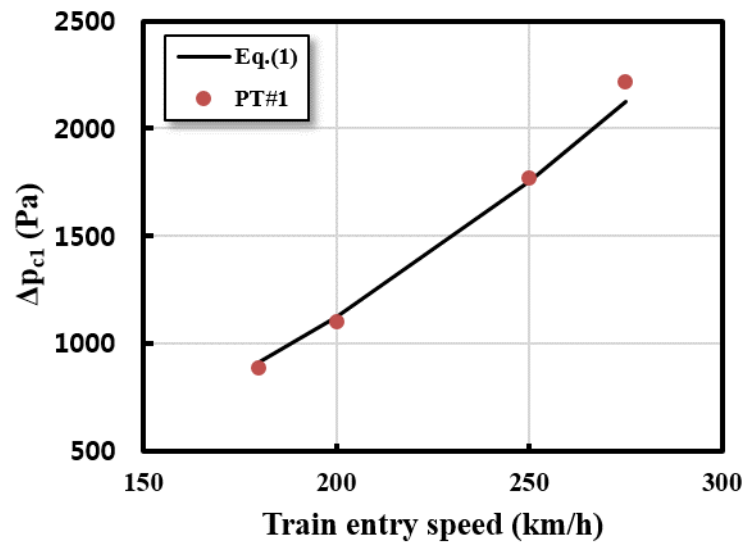
Figure 7: Relationship between the train entry speed V and the initial compression wave strength.

4 Conclusion

In this study, pressure measurement was performed inside the tunnel model to investigate the characteristics of the initial compression wave generated at the entrance of the tunnel model when the train model enters the tunnel model at high speed. The pressure waveforms near the tunnel model exit was different from the pressure waveforms at the tunnel model entrance due to the expansion wave reflected from the exit surface of the tunnel model. From the results of this study, the compression wave strength generated at the entrance of the tunnel also increased as the train model speed increased.

Acknowledgements

References

Kim HD (1994) Wave phenomenon in high-speed railway tunnel. *KSME* 34/10:796-807(in Korean)

Shigeru Haraasa (1960) Fluid dynamic problems when train enters tunnel at high speed. *NRRT* 153

Aoki T and Matsuo K (2000) Impulse sound emitted from high-speed railway tunnel exit. *6th Aeroacoustics Conference and Exhibit, Aeroacoustics Conferences, Lahaina, USA*

Baron A, Molteni P and Vigevano L (2006) High-speed trains: Prediction of micro-pressure wave radiation from tunnel portals, *Journal of Sound and Vibration* 296:59-72

Fukuda T, Saito H, Miyachi T, Kiduchi K and Iida M (2010) Experiments on the tunnel compression wave using an axisymmetric and three-dimensional train model. *Proceedings of the 10th International Workshop on Railway Noise* 419-426